Phy. Tomorrow Material Science Letters
2020; 27(04): 07-01.
https://www.wikipt.org/theoretical-physics-letters
doi:10.1490/p.ptl.2020.1564

Electrospun Strontium Titanata Nanofibers Incorporated with Nickel Oxide Nanoparticles for Improved Photocatalytic Activities

Abdulaziz Alharbi, Ibrahim M. Alarifi, Waseem S. Khan, and *Ramazan Asmatulu
Department of Mechanical Engineering
Wichita State University, 1845 Fairmount, Wichita, KS, 67260-0133
*Email: ramazan.asmatulu@wichita.edu

ABSTRACT

The inexpensive sources of fossil fuels in the world are limited, and will deplete soon because of the huge demand on the energy and growing economies worldwide. Thus, many research activities have been focused on the non-fossil fuel based energy sources, and this will continue next few decades. Water splitting using photocatalysts is one of the major alternative energy technologies to produce hydrogen directly from water using photon energy of the sun. Numerous solid photocatalysts have been used by researchers for water splitting. In the present study, nickel oxide and strontium titanata were chosen as photocatalysts for water splitting. Poly (vinyl pyrrolidone) (PVP) was incorporated with nickel oxide [Ni_2O_3] (co-catalyst), while poly (vinyl acetate) (PVAc) was mixed with titanium (IV) isopropoxide [$C_{12}H_{28}O_4Ti$] and strontium nitrate [$Sr(NO_3)_2$]. Then, two solutions were electrospun using coaxial electrospinning technique to generate nanoscale fibers incorporated with NiOx nanoparticles. The fibers were then heat treated at elevated temperatures for 2hr in order to transform the strontium titanata and nickel oxide into crystalline form for a better photocatalytic efficiency. The morphology of fibers was characterized via scanning electron microscopy (SEM), while the surface hydrophobicity was determined using water contact angle goniometer. The UV-vis spectrophotometer was also used to determine the band gap energy values of the nanofibers. This study may open up new possibilities to convert water into fuel directly using the novel photocatalysts.

Keywords: Electrospinning, Strontium Titanata, NiOx Nanoparticles, Calcination, Photocatalysts, Water Splitting.

1. INTRODUCTION

1.1 Water-Splitting for Hydrogen Production

Hydrogen is considered in a number of sectors as an ideal fuel of the future. This fuel can be yielded from clean and renewable energy sources; thus, its life cycle is clean and renewable in nature. Among the major sources of renewable energies, solar and wind are besides being promising sources for renewable energy production. Nevertheless, currently, renewable energy adds only about 5% of commercial hydrogen production predominantly through water electrolysis; on the other hand; 95% hydrogen is basically derived from fossil fuels, creating additional environmental concerns [1].

The electronic arrangement of a semiconductor plays a vital role in semiconductor photocatalysis. Contrary to a conductor, a semiconductor entails valance band (VB) and conduction band (CB). The energy difference existing between these two levels is said to be the energy band gap (Eg). Without any excitation, both the electrons and holes are in valence band. In the event that semiconductors are excited by photons with energy equivalent to or higher than their band gap energy level, electrons gain energy from the photons and are thus stimulated from VB to CB if the energy gain is higher than the band gap energy level [2]. In order to split water molecules utilizing a single photocatalyst, the band gap of a semiconductor has to interfere the reduction and oxidation potentials of water, which are +0 and +1.23 V, respectively, vs. a normal hydrogen electrode (NHE) at a zero reactant solution [3-5]. Figure 1 shows a schematic of comprehensive water splitting on a heterogeneous photocatalyst [6].

The elementary clue behind this research is to portray the $SrTiO_3$ nanofibers and to advance its properties by accumulating Ni_2O_3 nanoparticles which can be used as a photo catalyst for the production of hydrogen from water using solar energy, and thus improving the photocatalytic water splitting efficiency. As the photocatalytic water splitting requires a minimum band gap of 1.23 eV, NiO_3 possesses a large band gap of 3.85eV and is mostly transparent in the visible part of spectrum. Thus, Ni_2O_3 incorporated with $SrTiO_3$ nanofiber used as a catalyst can absorb the light and convert it into energy, which may be required for a water splitting.

Domen et al. reported the performance of NiO-loaded $SrTiO_3$ powders for hydrogen production from water. In this process, a reduction reaction of H_2 may be responsible for the NiO catalyst activation during the H_2 evolution, followed by O_2 oxidation to form a NiO/Ni double-layer structure. This process may possibly provide a further path for the electron migration from the photo catalyst to the catalyst surface. During these reactions, the NiO cocatalysts likely eliminate the back reaction between H_2 and O_2, which is completely different for Pt catalysts [7-10]. Many of different ternary titanates were developed and efficiently utilized for water splitting under UV irradiation. Shibata et al. reported that H_2 evolution from photocatalysts of layered structures of $Na_2Ti_3O_7$, $K_2Ti_2O_5$, and $K_2Ti_4O_9$ in aqueous methanol solutions using a Pt cocatalyst [11]. The quantum yield of $K_2Ti_2O_5$ materials obtained 10% efficiency. Several manufacturing procedures could provide some variations in photactivities of ternary metal oxides. The perovskite structure of $BaTiO_3$ (3.22 eV) prepared with a polymerized complex process has superior photocatalytic manner compared to traditional ways because of the various size, shape, and surface areas [12].

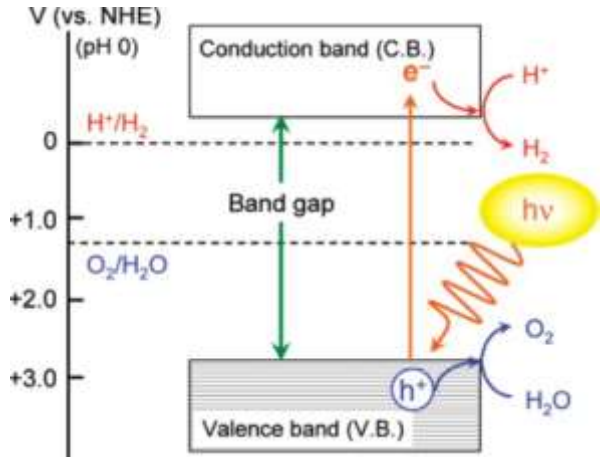

Figure 1: The schematic illustration of comprehensive water splitting on a heterogeneous photocatalyst [6].

1.2 Electrospinning

Electrospinning is used to create unremitting polymeric fibers with diameters stretching from few micrometers to few nanometers. The method involving electrospining is appropriate to virtually all naturally occurring polymers and synthetic polymers, polymer blends and polymers loaded with chromophores, nanoparticles, additives and metals and ceramics [13].These polymers can be adapted chemically and can be tailored with additives, such as carbon-black particles, enzymes, DNA, bacteria and viruses [13]. The distribution of metal nanoparticles into polymeric solution during electrospinning is of great significance owing to novel properties of nanocomposite fibers and due to continuous growing demand for miniaturization of electronic constituents, sensors, optical detectors and devices [14-15]. Electrospun nanofibers can be catalytic in comparison to conventional nanofiber membranes. Nanofibers based photocatalysts have higher surface area to volume ratio and its porous structure permit higher surface active sites for effective catalysis for many semiconductor applications [14].

2. EXPERIMENTAL

2.1 Materials

Toluene (99%) was purchased from Fisher Scientific, while poly (vinyl pyrrolidone) (PVP), poly (vinyl acetate) (PVAc, Mw = 500,000 g/mole), titanium (IV) isopropoxide, nickel oxide, and strontium nitrate (98%) were purchased from Sigma Aldrich. These materials and chemicals were used without any further purification or modification.

2.2 Method

Coaxial electrospinning refers to prolonged form of electrospinning. Coaxial electrospinning requires a central tube nozzle and a nozzle on outside of the central tube nozzle. In addition, two polymeric solutions for the core and sheath materials are separately fed into the central tube nozzle from which they are ejected simultaneously. A compound droplet develops from the central nozzle [16]. Figure 2 shows the image and schematic view of a

coaxial electrospinning process.

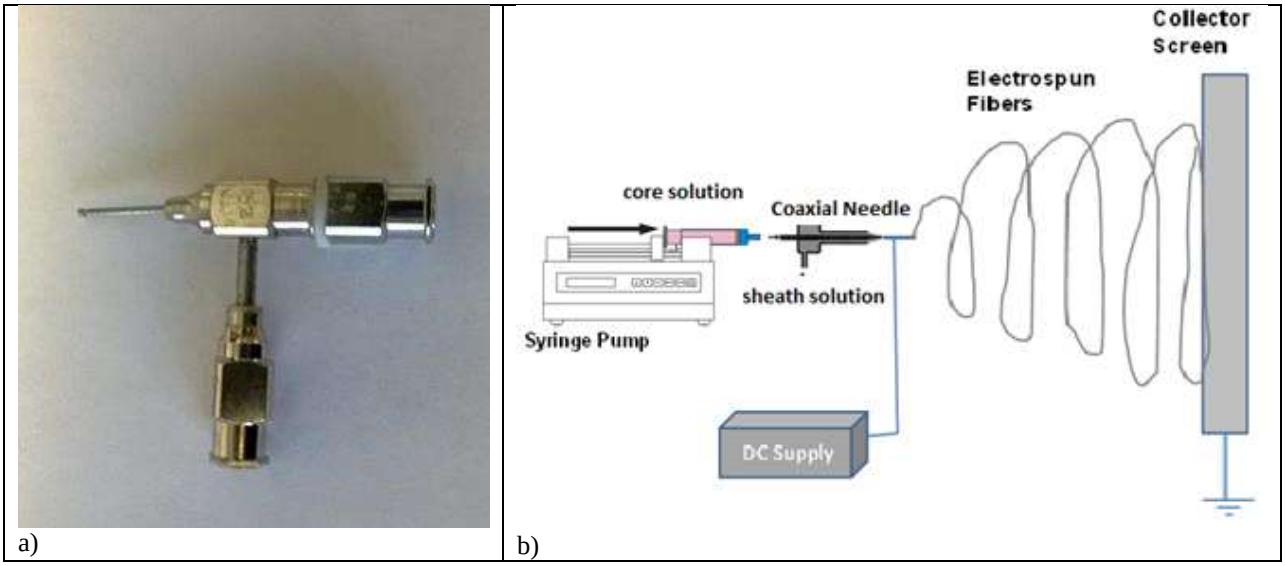

Figure 2: a) the image of coaxial needle, and b) schematic view of a coaxial electrospinning process.

In the instance that a high electrostatic field is applied, a multiple Taylor cone is realized that consists of core material surrounded by sheath material, and the jet experiences the same bending instability as in traditional electrospinning followed by evaporation. Finally, the jet becomes solid and is retrieved on a collector screen in the form of one fiber [17,18]. For this study, two polymeric solutions were prepared: the first one for the core and the second one for the sheath. For the core solution, poly (vinyl acetate) (PVAc) was dissolved in toluene with 10: 90 % weight ratios. Then, nearly 2% weight of titanium (IV) isopropoxide, and 2% weight of strontium nitrate were added slowly by stirring, and the resultant sol was stirred in a sealed beaker for 30 minutes. For the sheath solution, poly (vinyl pyrrolidone) (PVP) was dissolved in DI water with 10: 90 % weight ratios. Then, approximately 1% weight of nickel oxide, was carefully added, and the final sol was also stirred in a sealed beaker for 30 minutes. The two polymeric solutions were then poured into two different 10 ml syringes with 0.5 mm tip diameters. The first syringe was connected to the core nozzle on one side of the coaxial needle, whereas the second syringe was connected to the sheath nozzle on the other side of the coaxial needle. Both solutions were electrospun at 25 kV with a flow rate of 1 ml/hr. At a distance of 25 cm from the coaxial needle, which was used as the spinneret, an aluminum (Al) foil was used as a collector. These processes were arranged at room temperature. Finally, the Al foil with the nanofiber was kept in air to dry for several hours. Then the produced nanofibers were removed from the Al foil. The electrospun nanofibers were characterized using scanning electron microscopy (SEM) before and after the calcinations at 200, 260, and 300^{o} C for 2 hrs. It was assumed that the nanofibers could be in crystalline forms at lower temperatures and longer time than their bulk counterparts, which requires much higher temperatures.

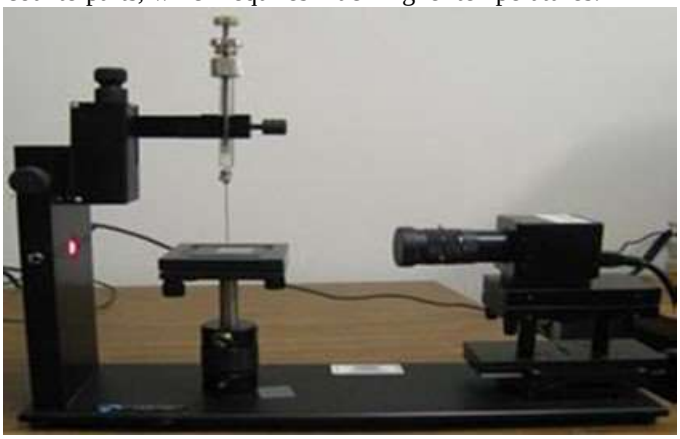

Figure 3: The photograph showing the optical contact angle goniometer used in the present study.

In order to measure the water contact angle values, an optical contact angle goniometer was chosen. It was purchased from KSV Instruments Ltd., Model #CAM 100. This goniometer is a compact video-based instrument that measures contact angles between 1º and 180º with an accuracy of 1º. Figure 3 shows the setting for this instrument. Band gap energy values of the prepared $SrTiO_3$ nanofibers incorporated with Ni_2O_3 nanoparticles were determined using UV-vis spectroscopy after grinding the fibers in a mortar grinder and dispersing in DI water well.

3. RESULTS AND DISCUSSION

3.1 SEM Analysis

SEM analysis were performed on the electrospun fibers to determine the surface morphologies of the fibers. A small portion of nanofiber films was cut and then sputter-coated with a nanolayer of gold for the SEM analysis. Figure 4 shows the SEM images of different electrospun nanofibers obtained at 25 KV DC voltage, 1 ml/h pump speed and 25 cm tip-to-collector distance. The images clearly show the variation in the fiber diameters, which may be because of fact that two different polymeric solutions were electrospun at the same time. The fiber diameters have a wide ranges of 180 nm to 2.18 µm, and they could be divided roughly into two groups of different sizes. This may be related to the viscosity differences of the prepared solutions and cleavage of the electrospinning jets while the fibers were developing [18]. In the second step, 1×2 inches of nanofiber samples were calcinated at 200, 260, and 300º C for 2 hrs. Figure 5 shows the SEM images of the samples after the heat treatment process. These images indicate that the nanofibers' mats had collapsed on the surface of the SEM holder, which may be due to the high temperature deformations of the organic fiber mats [19, 20].

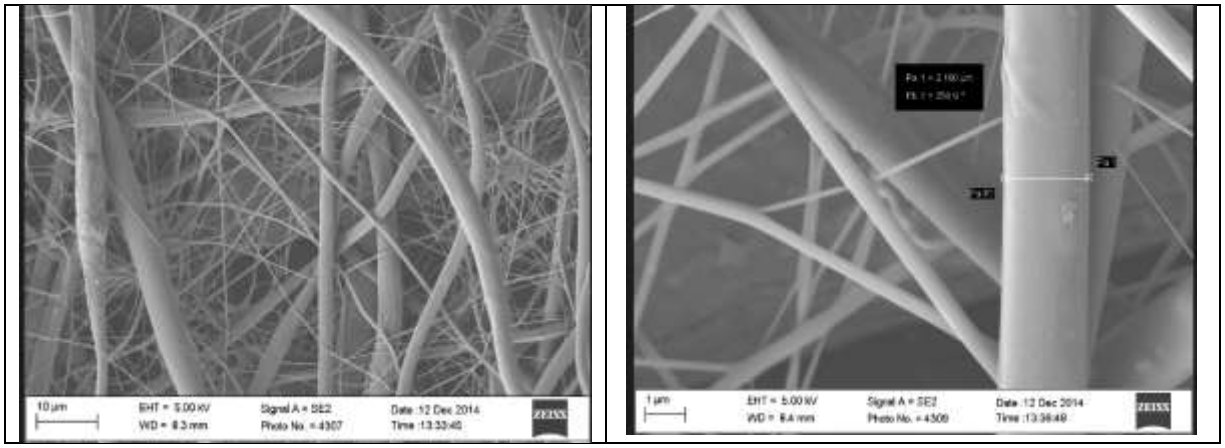

Figure 4: SEM images of the electrospun nanofibers obtained using coaxial needle at 25 KV DC voltage, 1 ml/h pump speed and 25 cm tip-to-collector distance prior to the calcination process.

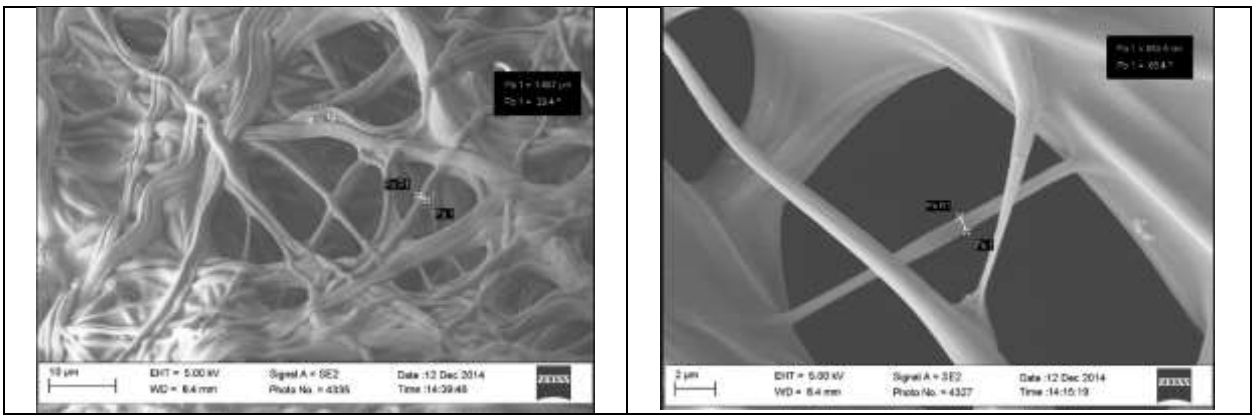

Figure 5: SEM images of the electrospun nanofibers after the calcination process.

3.2 Contact Angle Measurements

Water contact angle measurement is a proper way of determining surface hydrophobicity of the samples. Surface hydrophobicity values are significant in recognizing materials' wetting and adhesion characteristics. In this

research, two polymers were used to make the solutions. The first polymer was poly (vinyl pyrrolidone) (PVP), which is considered to be one of the most important synthetic polymers with perfect adhesion properties, less chemical toxicity and appropriate water solubility. PVP has an excellent wettability characteristic in respect to its high surface tension [21]. The appropriate solvents for dissolving poly (vinyl pyrrolidone) (PVP) for the electrospinning process are dimethylformamide, tetramethylammonium chloride, dichloromethane, and DI water [22-25]. The second polymer was poly (vinyl acetate) (PVAc), which shows great durability, availability, compatibility with other materials, and good adhesive properties [26]. The three nanofiber samples were put on glass specimen after the heat treatment at 200, 260, and 300º C for 2 hours, and then placed in front of the goniometer camera. A drop of DI water was then carefully released from a syringe needle onto the sample surface. Finally, the computer software recorded and measured the contact angle for each sample. Figure 6 shows the contact angle values of the prepared samples:

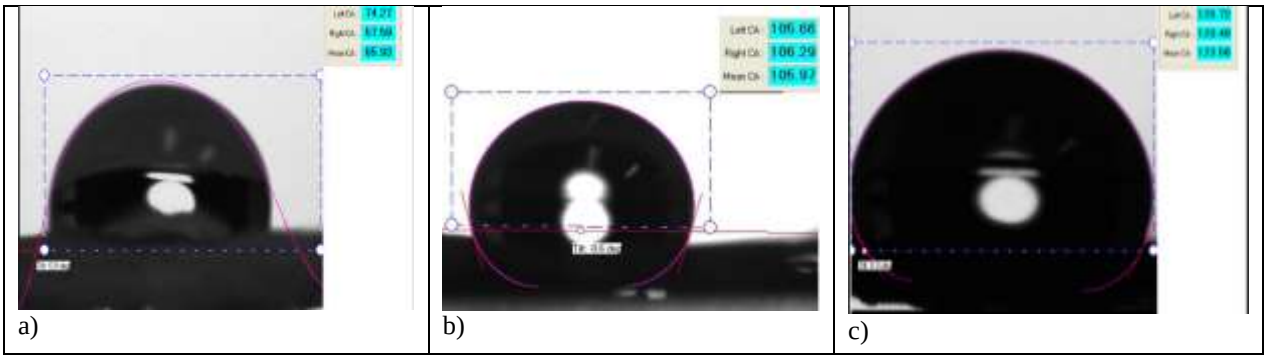

Figure 6. Water contact angle values of the nanofibers sample after heat treatments at a) 200 ºC, b) 260 ºC, and c) 300 ºC for two hrs.

The water contact angle values indicated that the sample has a hydrophilic surface after the heat treatment at 200 ºC. On the other hand, the samples given a heat treatment at 260 ºC, and 300º C have a hydrophobic surface. However, the highest result of the water contact angle was shown by the sample after the heat treatment at 300 ºC. For statistical purposes, each sample was tested at least 5 times and the results were averaged. Table 1 gives the water contact angel values of the electrospun nanofibers heat treated at 200, 260 and 300 °C.

Table 1: Water contact angel values of the electrospun nanofibers heat treated at 200, 260 and 300 °C.

Sample No.	Water Contact Angle (°)		
	200 ºC	260 ºC	300 ºC
1	74.27	105.66	126.72
2	61.24	109.62	114.12
3	86.38	105.97	126.13
4	76.69	106.82	115.05
5	88.01	105.17	125.11
Mean	77.31	106.64	121.42
St. Deviation	10.77	1.76	6.28

3.3 Measurement of Band Gap

In solar industries, it is vital to measure the band gap energy of materials, semiconductors, and nanomaterials. The simple method to determine the band gap of a material or a semiconductor is from its UV absorption spectrum. Insulators have large band gap energy (> 4eV) while semiconductors have lower band gap energy (< 3eV). However, it is not difficult to change the band gap properties of a semiconductor with the help of several semiconductor alloys [27-31]. In this study, two catalysts played an important role: strontium titanata and

nickel oxide (NiO_x). Nickle oxide is considered a wide band gap p-type semiconductor and is important for many researchers because of its magnetic and electrical properties. In addition to use as a catalyst, there are many attractive applications for (NiO_x) including use in gas sensors, supercapacitor electrodes, dye sensitized solar cells, and lithium ion batteries. The (NiO_x) has a band gap E_{gb}= 3.85 eV, while the ($SrTiO_3$) has a band gap E_{gb}= 3.25 eV. The UV spectrophotometer was used to determine the band gap energy of the produced nanofibers. Figure 7 shows the UV-Vis spectra curve of heat treated nanofibers suspended in DI water:

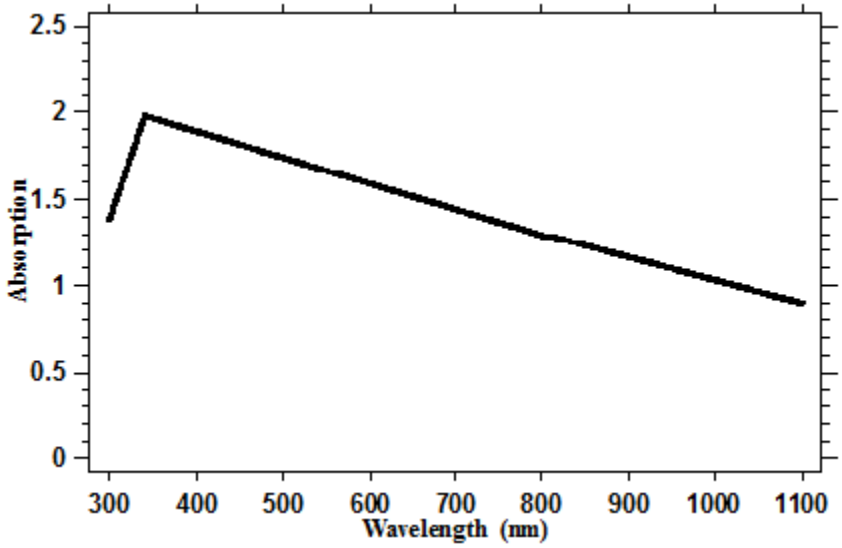

Figure 7: UV-vis spectra of an electrospun nanofibers heat treated at elevated temperature and suspended in DI water.

The band gap energy was calculated with the energy equation:

$$E = hc/\lambda$$

where h is Planck's constant (6.63 $x10^{-34}$ J.s.), c is the speed of light (3.00 $x10^{8}$m/s), λ is the wavelength (from Figure 7: λ= 340 nm). Using the energy equation above with the three parameters, the energy was found to be E= 5.85 $x10^{-19}$ J, which was then converted to E_{gb}= 3.65 eV. The ($SrTiO_3$) has a band gap E_{gb}= 3.25 eV; on the other hand, the (NiO_x) has a larger band gap E_{gb}= 3.85 eV. The measured band gap energy for the produced nanofibers was between the two values of the band gap energy for the $SrTiO_3$, and NiO_x. From Figure 7, it can be seen that the largest absorption peak of the calcinated sample appears at around 340 nm.

4. CONCLUSIONS

In this study, core/sheath nanofibers of $SrTiO_3$ and NiOx were produced by using the coaxial electrospinning method. Two catalysts were used: $SrTiO_3$ for the core and NiOx for the sheath. The electrospun nanofiber samples were heat treated at three different temperatures: 200, 260, and 300° C for 2 hrs. The morphology of fibers was observed by (SEM). The images clearly show two classifications of fiber diameters due to the two different electrospun polymeric solutions and cleaving process. The highest water contact angle value was found for the sample heat treated at 300° C for 2 hrs. The band gap energy for the produced nanofibers was calculated and the result showed a logical value: E_{gb}= 3.65 eV. These results may open up new possibilities to develop new nanoscale materials for water splitting.

ACKNOWLEDGMENT

The authors gratefully acknowledge the Kansas NSF EPSCoR (# R51243/700333) and Wichita State University for financial and technical support of the present work.

REFERENCES

1. Meng, N. I., Leung, M., Sumathy, K., & Leung, D. Y. C. "Water Electrolysis-a Bridge between Renewable Resources and Hydrogen," *Proceedings of the International Hydrogen Energy Forum,* 2004, Vol. 1, Beijing,PRC. pp. 475–480.
2. Ni, M., Leung, M. K., Leung, D. Y., & Sumathy, K. "A review and recent developments in photocatalytic water-splitting using TiO2 for hydrogen production," *Renewable and Sustainable Energy Reviews,* 2007, Vol. 11.3, pp. 401-425.
3. Kudo, A., & Miseki, Y. "Heterogeneous Photocatalyst Materials for Water Splitting," *Chemical Society Reviews,* 2009, Vol. 38.1, pp. 253-278.
4. Kitano, M., & Hara, M. "Heterogeneous Photocatalytic Cleavage of Water," *Journal of Materials Chemistry,* 2010, Vol. 20.4, pp. 627-641.
5. Youngblood, W. J., Lee, S. H. A., Maeda, K., & Mallouk, T. E. "Visible Light Water Splitting Using Dye-sensitized Oxide Semiconductors," *Accounts of chemical research,* 2009, Vol. 42.12, pp. 1966-1973.
6. Maeda, K., & Domen, K. "New Non-oxide Photocatalysts Designed for Overall Water Splitting under Visible Light," *The Journal of Physical Chemistry C,* 2007, Vol. 111.22, pp. 7851-7861.
7. Yokoi, T., Sakuma, J., Maeda, K., Domen, K., Tatsumi, T., & Kondo, J. N. "Preparation of a Colloidal Array of NaTaO3 Nanoparticles via a Confined Space Synthesis Route and its Photocatalytic Application," *Physical Chemistry Chemical Physics,* 2011, Vol. 13.7 pp. 2563-2570.
8. Kudo, A., Steinberg, M., Bard, A. J., Campion, A., Fox, M. A., Mallouk, T. E., ... & White, J. M. "Photoactivity of Ternary Lead-group IVB Oxides for Hydrogen and Oxygen Evolution," *Catalysis letters,* 1990, Vol. 5.1, pp. 61-66.
9. Sato, J., Kobayashi, H., Saito, N., Nishiyama, H., & Inoue, Y. "Photocatalytic Activities for Water Decomposition of RuO_2-loaded $AInO_2$ (A=Li, Na) with d^{10} Configuration," *Journal of Photochemistry and Photobiology A: Chemistry,* 2003**,** Vol. 158 (2-3), pp. 139-144.
10. Sato, J., Kobayashi, H., & Inoue, Y. "Photocatalytic Activity for Water Decomposition of Indates with Octahedrally Coordinated d10 Configuration. II. Roles of Geometric and Electronic Structures," *The Journal of Physical Chemistry B,* 2003. Vol. 107.31, pp. 7970-7975.
11. Shibata, M., Kudo, A., Tanaka, A., Domen, K., Maruya, K. I., & Onishi, T. "Photocatalytic Activities of Layered Titanium Compounds and Their Derivatives for H_2 Evolution from Aqueous Methanol Solution," *Chem. Lett.,* 1987**,** Vol. 16, pp. 1017-1018.
12. Yamashita, Y., Yoshida, K., Kakihana, M., Uchida, S., & Sato, T. "Polymerizable Complex Synthesis of $RuO_2/BaTi_4O_9$ Photocatalysts at Reduced Temperatures: Factors Affecting the Photocatalytic Activity for Decomposition of Water," *Chem. Mater,* 1998**,** Vol. 11 (1), pp. 61-66.
13. Greiner, A., & Wendorff, J. H. "Electrospinning: A Fascinating Method for the Preparation of Ultrathin Fibers," *Angew. Chem. Int. Ed.,* 2007, Vol. 46, pp. 5670 – 5703.
14. Mishra, S., Ahrenkiel, S. P. "Synthesis and Characterization of Electrospun Nanocomposite TiO2 Nanofibers with Ag Nanoparticles for Photocatalysis Applications," *Journal of Nanomaterials,* 2011, Vol. Article ID 902491, 6 pages.
15. Wang, Y., Li, Y., Sun, G., Zhang, G., Liu, H., Du, J., ... & Yang, Q. "Fabrication of Au/PVP Nanofiber Composites by Electrospinning," *Journal of Applied Polymer Science,* 2007, Vol. 105(6), pp. 3618–3622.
16. Khan, W. S., Asmatulu, R., Ceylan, M., and Jabbarnia, A. "Recent Progress on Conventional and Non-Conventional Electrospinning Processes," *Fibers and Polymers,* 2013, Vol. 14.8, pp.1235-1247.
17. Li, F., Song, Y., & Zhao, Y. "Core-Shell Nanofibers: Nano Channel and Capsule by Coaxial Electrospinning," *INTECH Open Access Publisher,* 2010.
18. Liu, H., & Tang, C. "Electrospinning of Cellulose Acetate in Solvent Mixture N, N-dimethylacetamide (DMAc)/Acetone," *Polymer journal,* 2007, Vol. 39.1 pp. 65-72.
19. Zhu, J., Wei, S., Chen, X., Karki, A. B., Rutman, D., Young, D. P., & Guo, Z. "Electrospun Polyimide Nanocomposite Fibers Reinforced with Core−Shell Fe-FeO Nanoparticles," *The Journal of Physical Chemistry C,* 2010, Vol. 114.19, PP, 8844-8850.
20. Hardman, S. J., Muhamad-Sarih, N., Riggs, H. J., Thompson, R. L., Rigby, J., Bergius, W. N., & Hutchings, L. R. "Electrospinning Superhydrophobic Fibers Using Surface Segregating End-Functionalized Polymer Additives," *Macromolecules,* 2011, Vol. 44, pp. 6461–6470.
21. Yang, Q., Li, Z., Hong, Y., Zhao, Y., Qiu, S., Wang, C. E., & Wei, Y. "Influence of Solvents on the Formation of Ultrathin Uniform Poly (vinyl pyrrolidone) Nanofibers with Electrospinning," *Journal of Polymer Science Part B: Polymer Physics,* 2004, Vol. 42, pp. 3721-3726.
22. Li, D., Wang, Y., & Xia, Y. "Electrospinning of Polymeric and Ceramic Nanofibers as Uniaxially Aligned Arrays," *Nano Letters,* 2003, Vol. 3(8), pp. 1167-1171.

23. Xie, J., Li, X., & Xia, Y. "Putting Electrospun Nanofibers to Work for Biomedical Research," *Macromol. Rapid Commun.*, 2008, Vol. 29, pp. 1775–1792.
24. Ignatova, M., Manolova, N., & Rashkov, I. "Novel Antibacterial Fibers of Quaternized Chitosan and Poly (Vinyl Pyrrolidone) Prepared by Electrospinning," *European Polymer Journal*, 2007, Vol. 43, pp. 1112–1122.
25. Li, L., Jiang, Z., Pan, Q., & Fang, T. "Producing Polymer Fibers by Electrospinning in Supercritical Fluids," *Journal of Chemistry*, 2013, pp. 1-6.
26. Yamak, H. B. "Emulsion Polymerization: Effects of Polymerization Variables on the Properties of Vinyl Acetate Based Emulsion Polymers," *INTECH Open Access Publisher*, 2013.
27. Dharma, J., Pisal, A., & Shelton, C. T. "Simple Method of Measuring the Band Gap Energy Value of TiO2 in the Powder Form Using a UV/Vis/NIR Spectrometer," *Application Note Shelton, CT: PerkinElmer*, 2009.
28. Theivasanthi, T., & Alagar, M. "Chemical Capping Synthesis of Nickel Oxide Nanoparticles and their Characterizations Studies," *arXiv preprint arXiv*, 2012, Vol. 1212.4595.
29. Lie, Y., Asmatulu, R. and Nuraje, N. "Photo-active Metal Oxide Nanomaterials for Water Splitting," (in press, *ScienceJet*).
30. Nuraje, N., Asmatulu, R., and Kudaibergenov, S. "Metal Oxide-based Functional Materials for Solar Energy Conversion: A Review," *Current Inorganic Chemistry*, 2012, Vol. 2, pp. 124-146.
31. Nuraje, N., Kudaibergenov, S., and Asmatulu, R. "Solar Energy Storage with Nanomaterials," in *Production of Fuels using Nanomaterials*, Taylor and Francis, Editor R. Luque and A.M. Balu, 2013, pp. 95-117.